THE PENNSYLVANIA STATE UNIVERSITY
SCHREYER HONORS COLLEGE

DEPARTMENT OF CHEMICAL ENGINEERING

Density Functional Theory analysis of clustering of ammonium, phosphonium, and
phosphazenium cations with fluoride and hydroxide anions

NICOLE LABARGE
Spring 2014

A thesis
submitted in partial fulfillment
of the requirements
for a baccalaureate degree
in Chemical Engineering
with honors in Chemical Engineering

Reviewed and approved* by the following:

Michael Janik
Professor of Chemical Engineering
Thesis Supervisor

Themis Matsoukas
Professor of Chemical Engineering
Honors Adviser

* Signatures are on file in the Schreyer Honors College.

ABSTRACT

Both batteries and fuel cells commonly rely on the exchange of cations in order to facilitate electrical current, using Li^+ in the case of batteries and H^+ in fuel cells. Anion exchange batteries and fuel cells, while not widely used, have the potential to address some main issues with their cation exchange counterparts. The main challenge for fluoride batteries and HEMFCs is to increase anion conductivity of the membrane. The focus of my research is to computationally evaluate cations for interactions with F^- and OH^- that indicate good conductivity in an anion exchange membrane. In addition to simple pairing, cations and anions can also combine to form aggregates. The possible ion states in the polymer system can be approximated using a four state model: free ions, ion pairs, quadrupoles, and triple ions. Ion pairs consist of a cation and anion; quadrupoles consist of two cations and two anions, arranged so that all interact; and triple ions can exist as negative triple ions, comprised of two anions and one cation, or positive triple ions, comprised of two cations and one anion. The relative affinities for the ions for each state have conductivity implications: quadrupoles impede ion mobility, while charged species promote charge transfer. Fluoride and hydroxide were paired with ammonium, phosphonium, and phosphazenium ions with varied substituents. Density Functional Theory calculations were used to evaluate the stability of the various ion clusters, informing the selection of cations that may offer optimal properties to facilitate anion conduction.

TABLE OF CONTENTS

LIST OF FIGURES

LIST OF TABLES

ACKNOWLEDGEMENTS

Chapter 1

Introduction

Much research, development, and production of batteries and fuel cells has revolved around those that facilitate transport of positive ions, such as H^+ and Li^+, between their electrodes. However, there are many potential advantages to pursuing technologies that instead use anion transport. Fluoride exchange batteries, which rely on the transport of fluoride ions between electrodes, are a promising technology for rechargeable batteries. They exhibit improved storage capacity and safety over lithium ion batteries; the high electronegativity and low weight of fluorine allow for a high theoretical battery potential [7]. Hydroxide exchange membrane fuel cells (HEMFCs) transport OH^- between their electrodes and address many current issues of proton exchange fuel cells. The basic environment of HEMFCs better facilitates oxygen reduction at the cathode, which increases efficiency by decreasing cathode over-potential [12]. The half-reactions that occur have less need for the precious metal catalysts used in proton exchange fuel cells [8]. Instead, metals such as Fe, Co, and Ni can be used in HEMFCs [2].

A major design consideration in batteries and fuel cells is the medium through which the charged species is transported. Previously developed hydroxide exchange fuel cells used liquid electrolytes for this purpose; carbon precipitates in the electrolyte were formed due to impure hydrogen feeds [1]. The use of polymer membranes, consisting of cations attached to a polymer backbone, minimizes this issue. Conductivity of these Anion Exchange Membranes (AEMs) is a main limiting factor for this technology,

especially when compared to well-established proton exchange membranes (PEMs) [8]. Because of the inherent lower conductivity of OH$^-$ over H$^+$, greater ion exchange capacity (IEC) or greater number of cationic sites is often required to attain comparable conductivity – IECs of AEMs are typically 2 to 3 times that of PEMs [8]. Polymer degradation of the attached cations in the basic media is another issue to consider, though we neglect this factor in this study [1], [2], [4]. The necessarily increased IECs also lead to increased degradation via Hoffman elimination.

The cations used in this experiment include a set of phosphonium and ammonium ions, as these are more widely studied and display reasonable stability [3], [4], [5]. Ammonium AEMs have been found to be more stable than phosphonium AEMs [3]. This concern lead to investigation into different cationic species to test. Despite the trend of low phosphonium stability, Yan et al derived an AEM with tris(2,4,6-trimethoxyphenyl)phosphonium (TPQPOH) units that shows favorable stability and conductivity [5]. Phosphazenium was studied as an alternative to phosphonium and ammonium.

This study seeks to help fill a knowledge gap on AEM conductivity to aid in choosing cations for these polymers. The associations between attached cations and anions in this polymer system are complex; therefore, analysis was simplified by using a four-state model of ion aggregation in ionic polymer systems introduced by Shiau et al (Figure 1) [9]. Free ions and triple ions represented charged species that contribute to anion conduction. The other two states, pairs and quadrupoles, have implications on ion mobility; a comparison of the energies of each state represent a cation's tendency to aggregate and form cross-links in the polymer, which could decrease conductivity.

Choosing an optimal cation for the ionomer will allow anion dissociation and avoid agglomeration in large clusters.
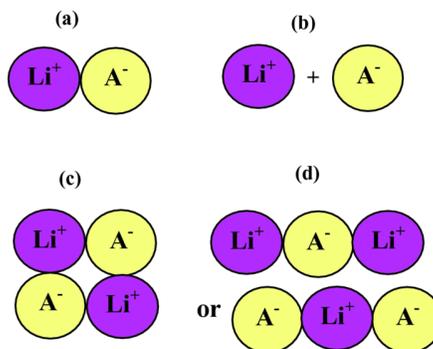
Figure 1. Schematics of four ion states (a) ion pairs; (b) separated ions (free); (c) quadrupoles; and (d) triple ions (negative and positive triple ions) composed of an anion (pictured here as A^-) and a cation (pictured here as Li^+) [9]

Density Functional Theory (DFT) was used to measure the interactions within the four states that impact performance. Ab initio calculations were performed using the Gaussian03 software using the B3LYP functional with the 6-31 +g(d) basis set. The choice of B3LYP was supported by its use in similar studies, both on cation-transporting species [6] and studies on cation-anion interactions and polymer degradation in AEMS [2].

Herein, I explore the conductivity of AEMs through analyzing the interactions between the anions and the cations attached to the membrane using DFT. Energies obtained for simple aggregates were used to suggest their impact on conductivity of a membrane containing the given ion by observing implications of the data on aggregate formation and charge mobility. The interactions between cations and anions were studied using the four state model, looking solely at the interaction between the ions in a gas phase model and neglecting longer range polymer interactions, or solvation. The

interactions between F^- and OH^- anions and phosphonium, ammonium, and phosphazenium cations were studied to compare trends in aggregate stability.

Chapter 2

Methods

Four state model

The cation groups attached to the polymer backbone were studied as the primary ionomer component responsible for conduction. This project focused on the interactions between the cation groups and the anions responsible for transporting charge through the membrane. Fluoride was studied for battery applications, and hydroxide for fuel cell applications. The extended polymer beyond the cation functional group was not included in the model. Discussion of solvation by the extended polymer or entropic implications of aggregation and their impact on state stability can be found in Shiau et al [9]. The goal of the study discussed herein was to study the interaction differences among cation/anion combinations, which are well captured by the simple "gas phase" ion models used.

In addition to cation-anion pairs, larger aggregates can be found within an ionomer. While large aggregates can form, a four-state model was used to more concretely compare cations. These states were separated ions, ion pairs (+,-), triple ions (+,-,+ or -,+,-), and quadrupoles (+,-,+,-). Conductivity was assumed to be a product of the concentration of charged species and the mobility of species; comparisons of energies of each form yield insight into these two considerations. In application, the solvating environment would inhibit formation of large aggregates, justifying the use of this simplification.

Computational methods

Gaussian 03 was used to perform ab initio calculations to find the energies of each state via Density Functional Theory (B3LYP functional) with the 6-31+G(d) basis set. Quantum mechanical methods of calculation are an appropriate choice in evaluating ion interactions for improved ionomer design. DFT can be used to quickly obtain accurate assessments of the interactions of polymer functional groups with ions. The binding energies for the four states were calculated with equations 1-4.

$$\Delta E_{pair} = E_{anion} + E_{cation} - E_{pair} \quad (1)$$

$$\Delta E_{triple+} = E_{anion} + 2 \times E_{cation} - E_{triple+} \quad (2)$$

$$\Delta E_{triple-} = 2 \times E_{anion} + E_{cation} - E_{triple-} \quad (3)$$

$$\Delta E_{quadrupole} = 2 \times E_{anion} + 2 \times E_{cation} - E_{quadrupole} \quad (4)$$

A more positive value of ΔE_{state} indicates greater stability of the state relative to the separated anions and cations. Triple ion factor and quadrupole factor were used as an indication of the tendency to form charged states that participate in conduction or tendency of the ions to cluster (Equations 5-6). The quadrupole factor approximates the likelihood of quadrupole formation from two pairs, while the triple ion factor approximates triple positive and triple negative formation from three pairs. A small quadrupole factor indicates greater mobility due to less clustering, and a large triple ion factor indicates a greater concentrations of charged species that enhance charge transfer. Both low quadrupole factor and high triple ion factor imply greater conductivity.

$$Quadrupole\ Factor = \frac{\Delta E_{quadrupole}}{2 \times \Delta E_{pair}}\ (5)$$

$$Triple\ Ion\ Factor = \frac{(\Delta E_{triple+} + \Delta E_{triple-})}{3 \times \Delta E_{pair}}\ (6)$$

Cations tested

Ammonium, phosphonium, and phosphazenium ions were examined.

Ammonium and phosphonium ions with methyl, ethyl, and propyl substituent chains

were compared. Phosphazenium (PPM) was compared to phosphazenium with an

ethylene glycol side chain (PPME) to approximate solvation of the ions by the

polyethylene oxide backbone (Table 1).

Table 1. Cations tested

Ammonium	TMA (Tetramethyl Ammonium)	TEA (Tetraethyl Ammonium)	TPA (Tetrapropyl Ammonium)
Phosphonium	TMP (Tetramethyl Phosphonium)	TEP (Tetraethyl Phosphonium)	TPP (Tetrapropyl Phosphonium)
Phosphazenium	PPM (Phosphazenium)	PPME (Phosphazenium with ethylene glycol side chain)	
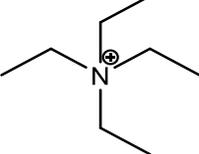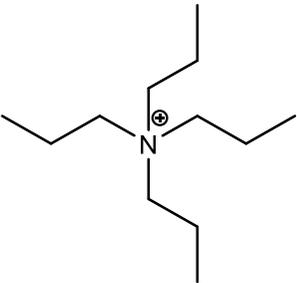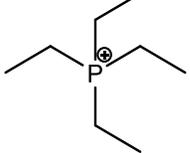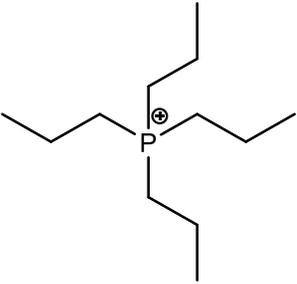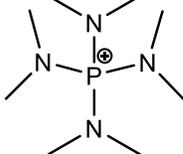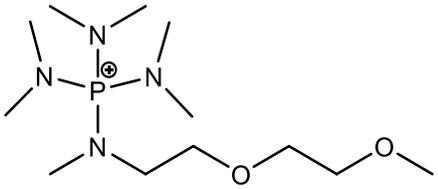
Dipole-dipole analysis

Lowest-energy quadrupole structures were comprised of two pair structures. The contributions of pair dipole/pair dipole interactions to quadrupole formation was studied via the following approximations. The pairs were approximated as two point charges of equal magnitude to determine a charge that matched the calculated pair dipole moment. We assumed this point charge to be localized on the central atom in the cation, and on the oxygen in hydroxide. The charge on each ion in the dipole pair was calculated from the dipole moment of the pair as well as the distance between the central cationic atom and the anion in the paired state. The dipole-dipole interaction energy of the quadrupole was calculated using these pair-calculated charges and the ion positions. The dipole-based interaction energy was compared to the quantum derived quadrupole interaction energy.

Chapter 3

Results and Discussion

Table 2 and Table 3 report all four state formation energies used in the subsequent calculations discussed below. We observe from the binding energies that F^- pair, triple ion, and quadrupole states are less stable than hydroxide aggregates. Most pair, triple, and quadrupole energies are larger, indicating stronger binding, for phosphonium than ammonium, though there are exceptions. Phosphazenium energies were in the range of ammonium values.

Table 2. Gas-phase binding energies for F⁻ with various cations in the four states (kJ/mol)

		ΔE_P	ΔE_{T+}	ΔE_{T-}	ΔE_Q
Ammonium					
TMA	Tetramethyl ammonium	476	636	632	1047
TEA	Tetraethyl ammonium	435	571	589	951
TPA	Tetrapropyl ammonium	427	555	580	928
Phosphonium					
TMA	Tetramethyl phosphonium	531	626	626	1078
TEA	Tetraethyl phosphonium	499	584	597	1005
TPA	Tetrapropyl phosphonium	488	569	589	985
Phosphazenium					
PPM	Phosphazenium	457	523	571	915
PPME	Phosphazenium with ethylene glycol side chain	461	539	572	924

Table 3. Gas-phase binding energies for OH⁻ with various cations in the four states (kJ/mol)

		ΔE_P	ΔE_{T+}	ΔE_{T-}	ΔE_Q
Ammonium					
TMA	Tetramethyl ammonium	493	626	642	1073
TEA	Tetraethyl ammonium	451	566	595	957
TPA	Tetrapropyl ammonium	443	548	588	928
Phosphonium					
TMA	Tetramethyl phosphonium	544	613	677	1131
TEA	Tetraethyl phosphonium	513	573	622	1053
TPA	Tetrapropyl phosphonium	502	558	600	1030
Phosphazenium		544	613	677	1131
PPM	Phosphazenium	477	509	632	972
PPME	Phosphazenium with ethylene glycol side chain	484	525	635	972

Quadrupole Factors

The quadrupole factors of the cations with fluoride or hydroxide show the likelihood of an ion to adopt the quadrupole versus the paired state. All ions tested had quadrupole factors greater than unity, indicating that the additional interactions in the quadrupole compared to the paired state stabilize the aggregate. A quadrupole factor close to unity indicates minimal enthalpic preference for the quadrupole state over the paired state. Increasing the size of the substituent was anticipated to lower the quadrupole factor by sterically preventing close binding of the cation and anion. To test the effect of larger substituent groups, three tetrahedral ammonium ions and three tetrahedral phosphonium ions were tested with methyl, ethyl, and propyl substituents (Figure 2, Figure 3, Figure 4, Figure 5).

Phosphonium ions bind more tightly to the anion than ammonium. In the pair, tetrahedral phosphonium adopts a more planar configuration, allowing the anion to interact more closely with the central positively charged phosphorous, which can be expected due to the lower electronegativity of phosphorous versus nitrogen. This can be seen by comparing the distance between the central cationic atom and either fluoride or hydroxide in the pair; the bonding distance for phosphonium is approximately 1.8 Å, while the distance for ammonium is 3.0 Å. As the ions in the phosphonium pair are more closely bound than that of ammonium, there is less of an increased stabilization of the quadrupole. This can be assessed quantitatively by comparing dipole moments of the
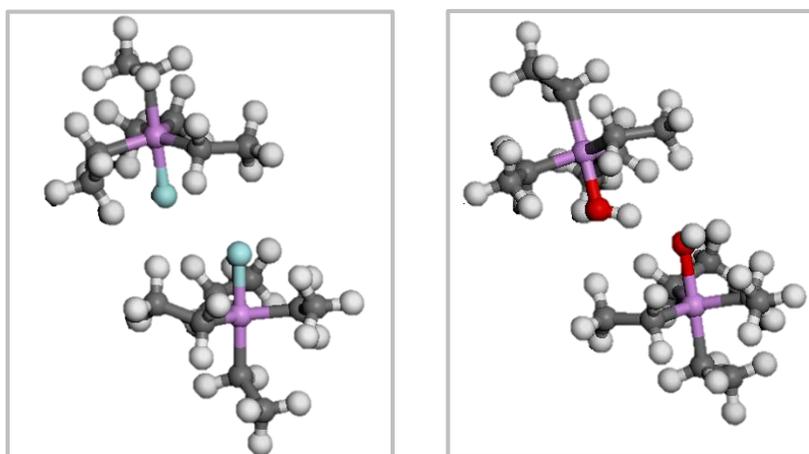
pair structure. The effect of dipole-dipole binding in increasing the quadrupole factor, particularly for ammonium, is discussed further on p. 9.
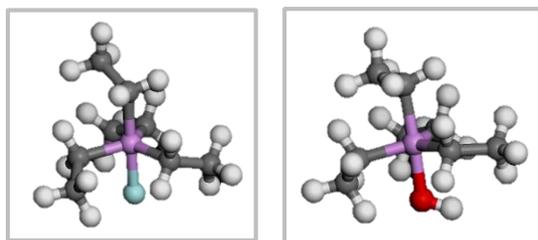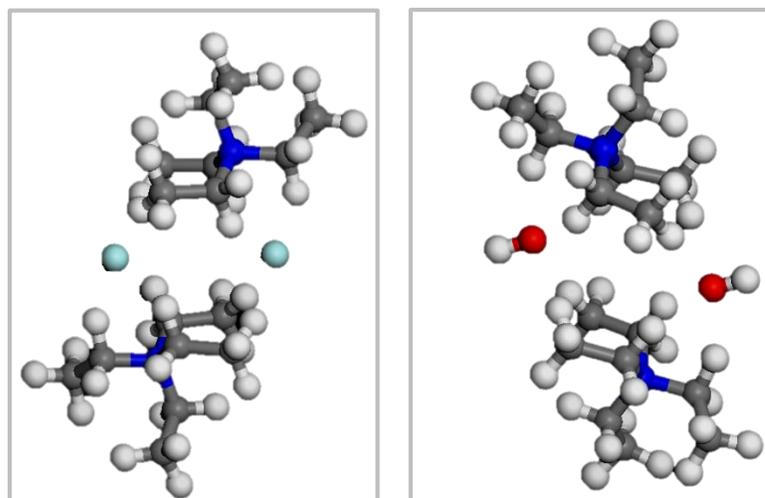

Figure 2. Paired structures for tetraethyl phosphonium with fluoride (left) and hydroxide (right)
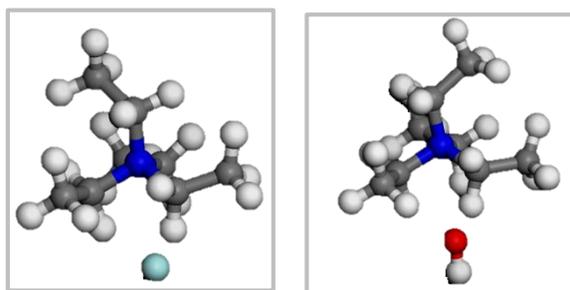
Figure 3. Paired structures for tetraethyl ammonium with fluoride (left) and hydroxide (right)

**Figure 4. Quadrupole structures for tetraethyl phosphonium with fluoride (left) and hydroxide (right)**

Figure 5. Quadrupole structures for tetraethyl ammonium with fluoride (left) and hydroxide (right)

The quadrupole factors for all ions tested were lower for phosphonium than for ammonium, reflecting the stronger and closer phosphonium pair binding and therefore lessened energy stabilization for the quadrupole. A clear decrease in quadrupole factor with increasing alkyl chain length can be seen for ammonium (Figure 6, Figure 7). As chain length is increased, charge is distributed across more atoms in the cation. There is

therefore less of an energy benefit of quadrupole formation from the paired state as chain length increases. The same decreasing quadrupole factor with increasing chain length can be observed for phosphonium with hydroxide, but not with fluoride.
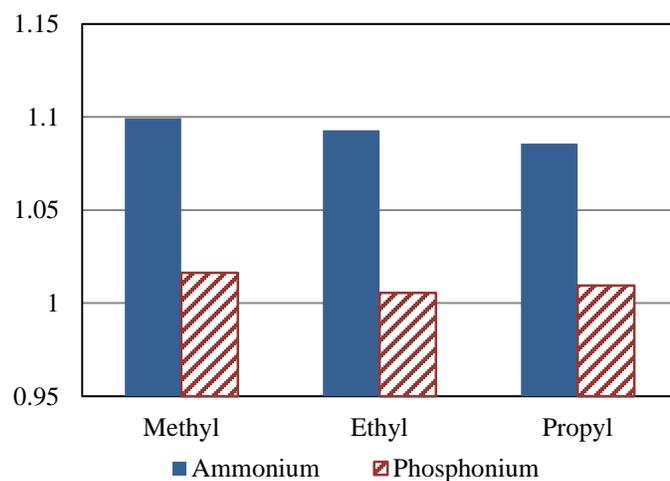

Figure 6. Quadrupole factors for fluoride and ammonium or phosphonium with four methyl, ethyl, or propyl substituents
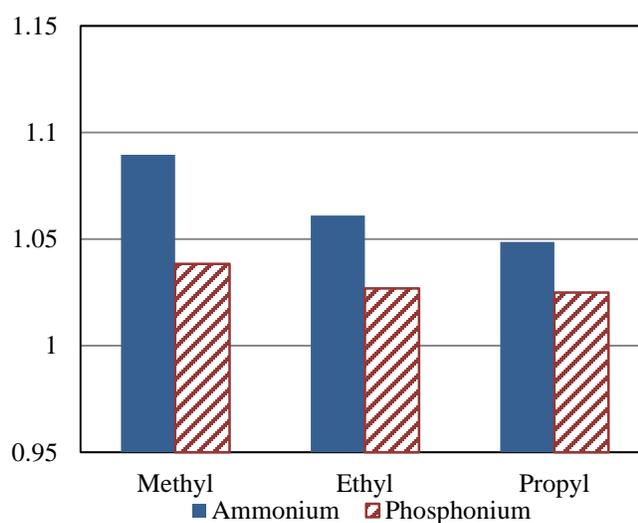

Figure 7. Quadrupole factors for hydroxide and ammonium or phosphonium with four methyl, ethyl, or propyl substituents

Phosphazenium was studied with the anticipation that its greater steric hindrance and increased charge delocalization would decrease the quadrupole factor. Phosphazenium with an ethylene glycol side chain was tested to simulate solvation by the polymer backbone. Phosphazenium, like phosphonium, adopted a planar configuration in the pair and in the quadrupole (Figure 8, Figure 9), as did phosphazenium with an ethylene glycol chain (Figure 10, Figure 11). The additional solvation did not have a great effect on phosphazenium's interaction with fluoride, but yielded a visible decrease in quadrupole factor for the ion with hydroxide.
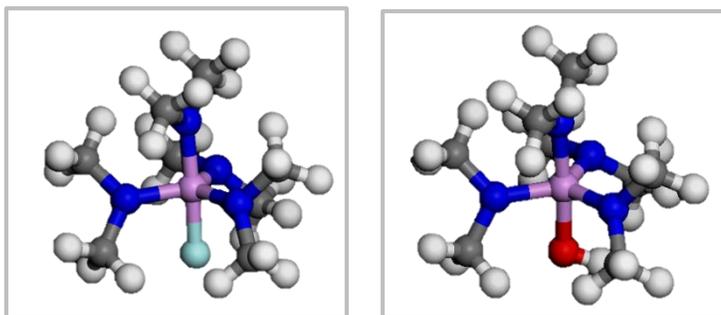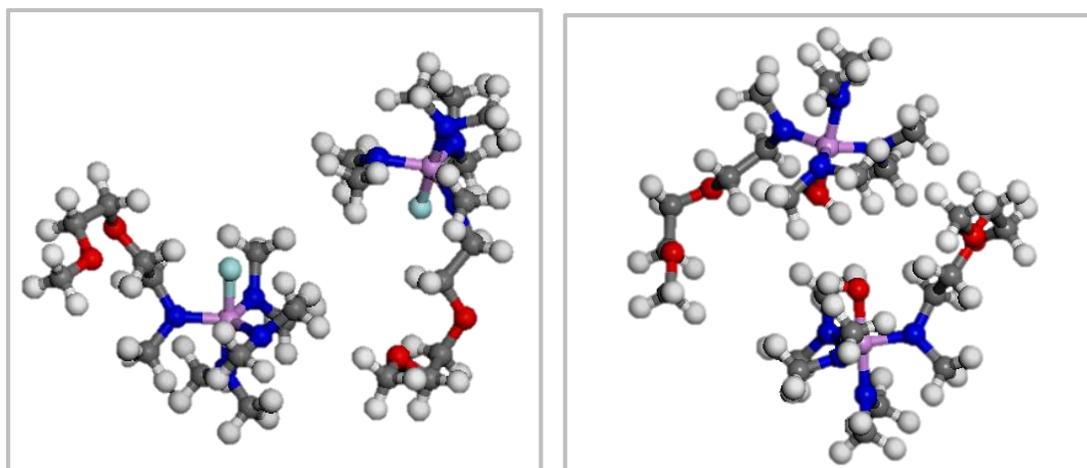

Figure 8. Paired structures for phosphazenium with fluoride (left) and hydroxide (right)
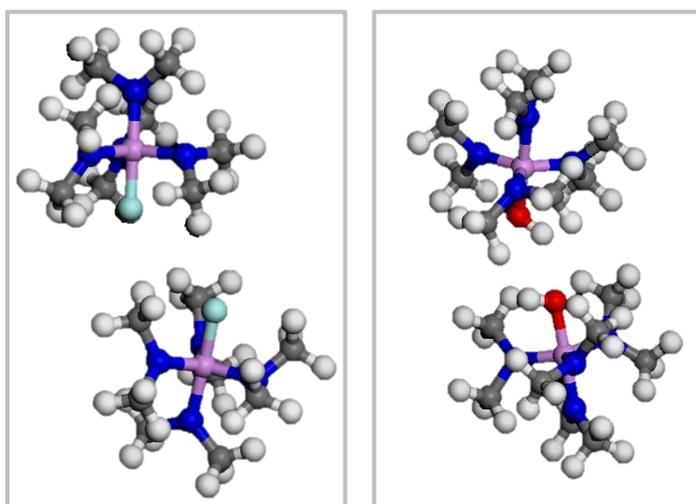
Figure 9. Quadrupole structures for phosphazenium with fluoride (left) and hydroxide (right)
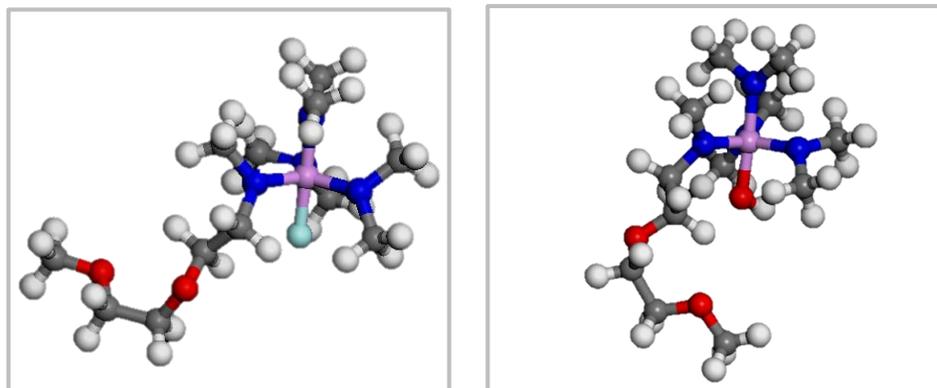
Figure 10. Paired structures for phosphazenium having an ethylene glycol chain with fluoride (left) and hydroxide (right)

Figure 11. Quadrupole structures for phosphazenium having an ethylene glycol chain with fluoride (left) and hydroxide (right)

With electronegative nitrogen atoms interacting directly to the central phosphorous in phosphazenium, the distance between the anion and central cationic P atom decreased as compared to phosphonium pairs: from 1.88 to 1.76 Å for tetrapropyl phosphonium to phosphazenium with fluoride, and from 1.87 to 1.77 Å for tetrapropyl phosphonium to phosphazenium with hydroxide. As expected, the more stable pairs

formed for phosphonium resulted in slightly lower quadrupole factors (Figure 12, Figure

13).
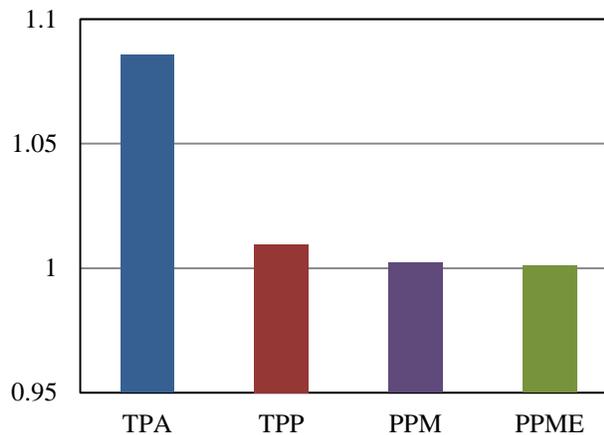
Figure 12. Quadrupole factors of fluoride with (left to right) tetrapropyl-ammonium, tetrapropyl-phosphonium, phosphazenium, and phosphazenium with an ethylene glycol side chain.
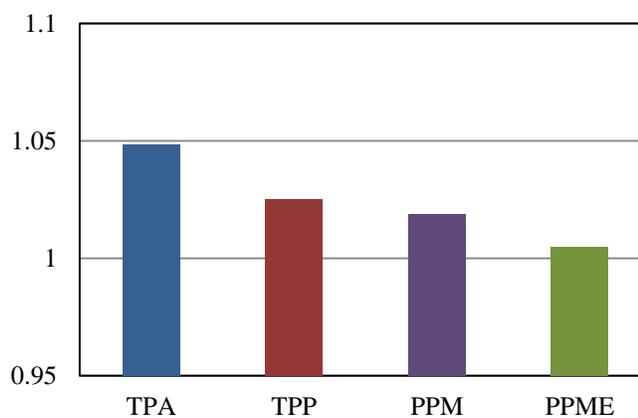
Figure 13. Quadrupole factors of hydroxide with (left to right) tetrapropyl-ammonium, tetrapropyl-phosphonium, phosphazenium, and phosphazenium with an ethylene glycol side chain.

A graph of the quadrupole binding energy versus twice the pair binding energy

graphically displays the quadrupole factor, with increasing quadrupole factor moving

farther above the 45 degree line (Figure 14, Figure 15). Quadrupole factor for

phosphazenium is closest to unity, followed by phosphonium and then ammonium.

Generally, cations with longer substituent chains can adopt lower energy structures, whether quadrupole or pair, indicating looser cation-anion binding. However, this does not necessarily indicate a lower quadrupole factor.
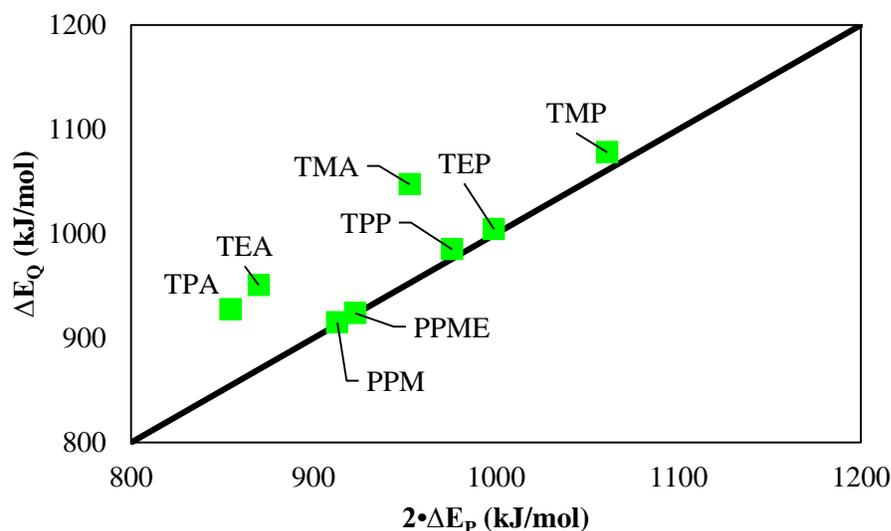
Figure 14. Quadrupole factor for cations with F⁻: Formation energy of the quadrupole versus twice the formation energy of the pair
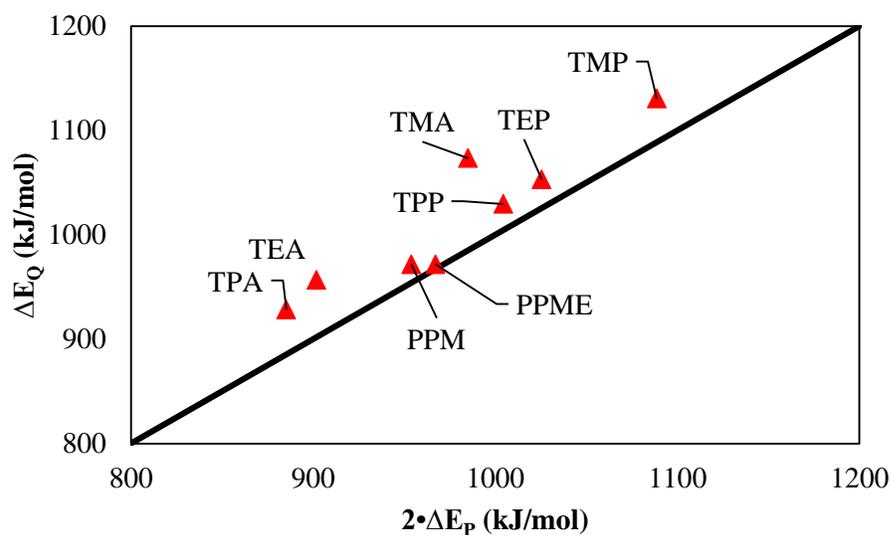

Figure 15. Quadrupole factor for cations with OH⁻: Formation energy of the quadrupole versus twice the formation energy of the pair

To summarize the analysis of quadrupole factors: Stronger pair binding in phosphonium leads to less tendency to form a quadrupole than ammonium. We expect less agglomeration into larger clusters in phosphonium ionomers, though stronger pairing suggests less free charges. Phosphazenium seems to better balance these two interactions, as pair binding energies are closer to ammonium, yet their quadrupole factors are lower. This suggests that phosphazenium may resist clustering like phosphonium, but also allow for free charge formation.

Effect of Dipole-Dipole interactions on Quadrupole Factors

As mentioned previously, quadrupoles can be thought of as forming from two pairs; all four ions are interacting, but those interactions can be seen as that between two distinct dipoles created by each pair. Ammonium pairs, with their greater charge separation, were hypothesized to be characterized by greater dipole moments, which would explain the increased stabilization of quadrupole formation over phosphonium. Phosphoniums have a shorter cation-anion distance, more electron sharing, and therefore a smaller dipole moment.
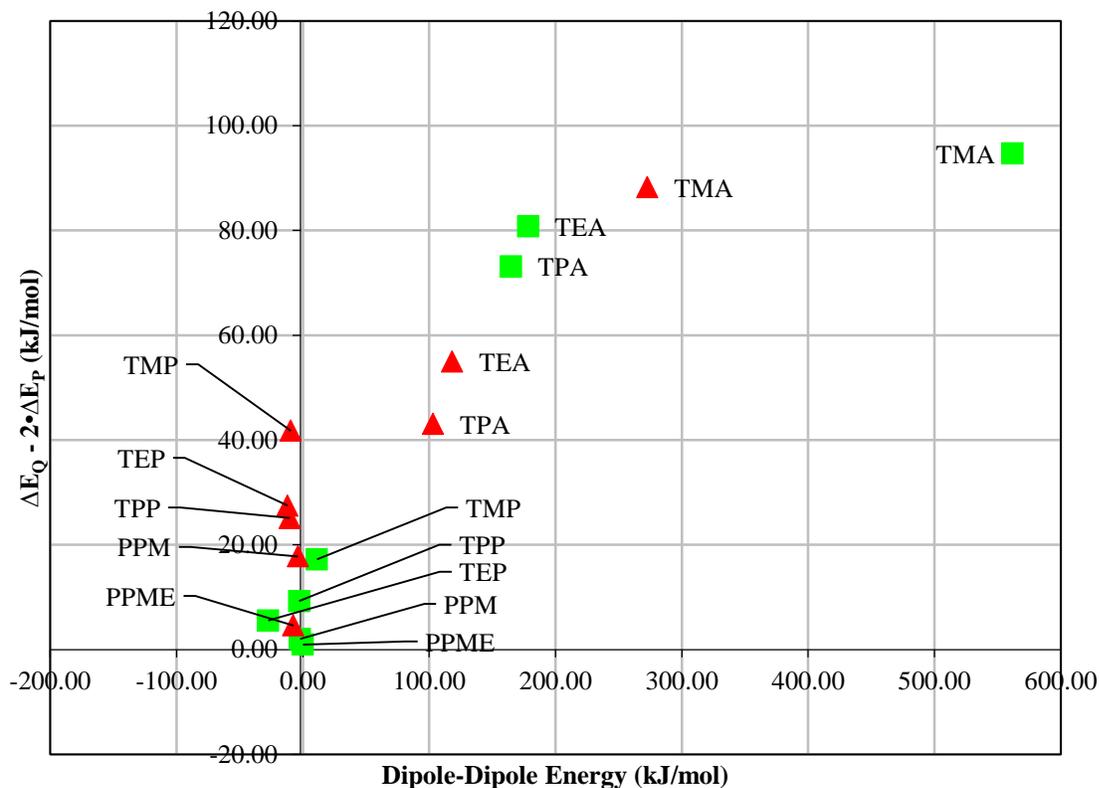
The formation energy of a quadrupole from two pairs was first plotted against the pair dipole moment as calculated by Gaussian (Figure 16). As anticipated, higher dipole moments correlated roughly linearly with higher quadrupole-from-pair formation energy, indicating an increased affinity for aggregation. For phosphonium ions, quadrupole-from-pair energy ($\Delta E_Q - 2 \cdot \Delta E_P$, y-axis Figure 16) for a given dipole moment is higher for hydroxide aggregates than fluoride. This is likely due to added stabilization in the quadrupole due to hydrogen binding between pairs that is not seen in the pair dipole moment. Among phosphonium or ammonium with fluoride or hydroxide, increased alkyl chain length decreases both the quadrupole-from-pair energy and the dipole moment; larger substituents promote greater charge delocalization and introduce steric repulsions in the quadrupole state.
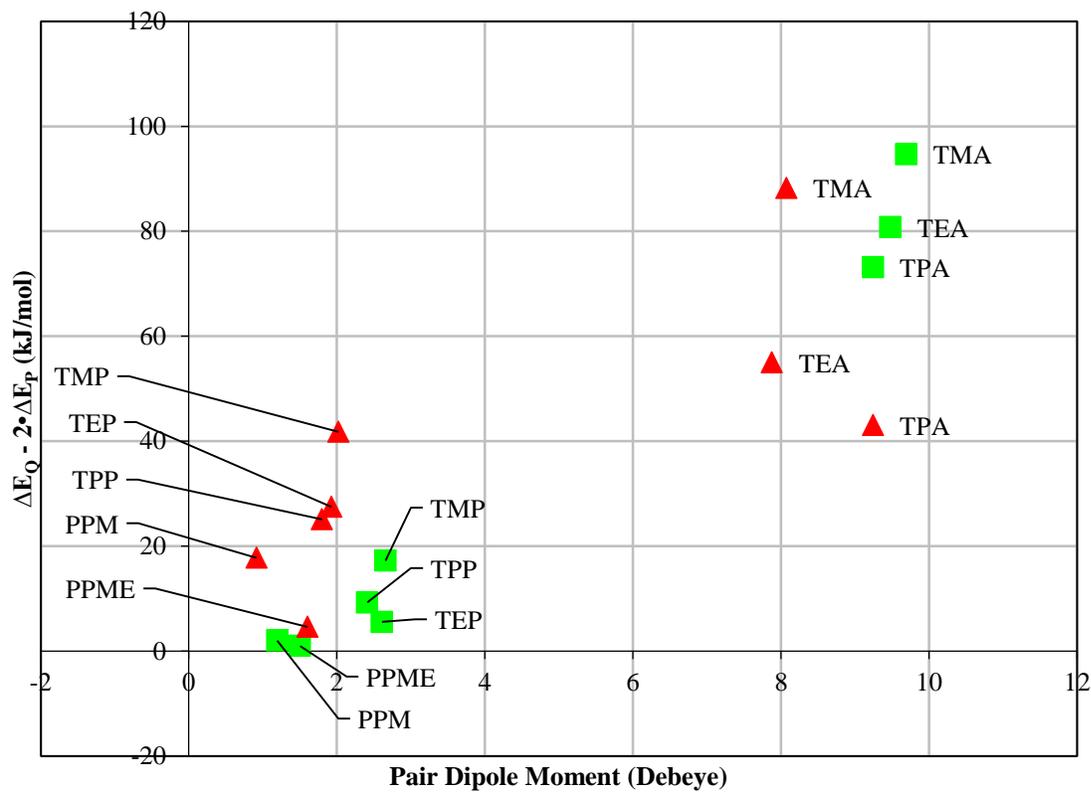
Figure 16. Quadrupole formation energy from two pairs versus dipole moment of the pair. Red triangles represent hydroxide systems, and green squares represent fluoride systems.

Next, the dipole moment and cation-anion distance was used to calculate the energy of quadrupole formation from two pairs considering only the dipole-dipole interaction of the pairs (Figure 17). The pair-pair interaction energy in the quadrupole is calculated from an approximate dipole-dipole interaction (x-axis Figure 17) and from the full quantum calculation (y-axis Figure 16). From this graph, it is clear that the dipole-dipole interactions of phosphonium and phosphazenium are negligible. Lack of significant dipole-dipole interactions allows the quadrupole factors associated with these cations to be near 1. Quadrupole formation of ammonium systems can be explained via dipole-dipole analysis, as ammonium pairs experience greater charge separation and

therefore a stronger dipole moment. The relationship between increased alkyl chain

length and both decreased quadrupole-from-pair binding energy and decreased dipole-

dipole interaction energy is clear among ammonium systems.

Figure 17. Quadrupole formation energy from two pairs versus dipole-dipole energy of the quadrupole state. Red triangles represent hydroxide systems, and green squares represent fluoride systems.
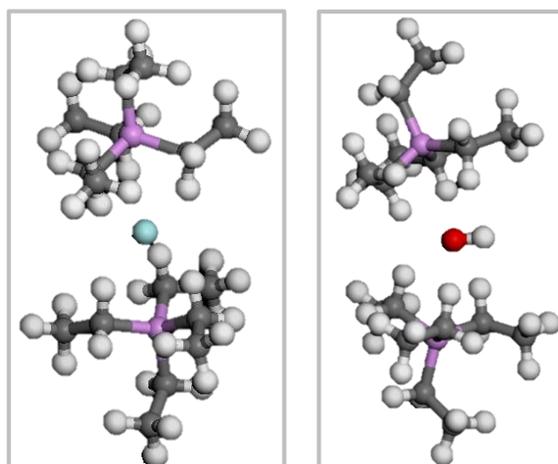
Triple Ion Factors

Triple ion factors compare the likelihood of a cation and anion to form charge-conducting triple positive or triple negative species to the likelihood of the formation of paired species. Therefore, high triple ion factors suggest a greater tendency to form charged species that may participate in conduction. While all factors are less than unity because charged species are necessarily less stable than charge-neutral species, they follow similar trends to the quadrupole. Examples of phosphonium and ammonium triple negative (Figure 18, Figure 19) and triple positive (Figure 20, Figure 21) structures are shown. Tetraethyl phosphonium and ammonium structures are given in the figures, and tetramethyl- and tetrapropyl- cations show similar trends. The octahedral triple negative phosphonium/hydroxide structure is consistent across all tests.
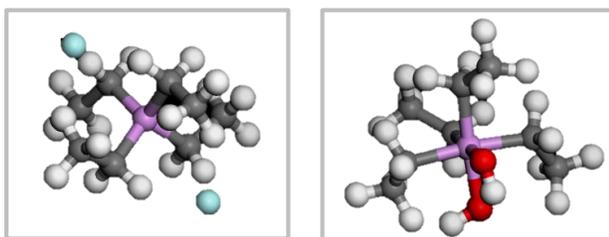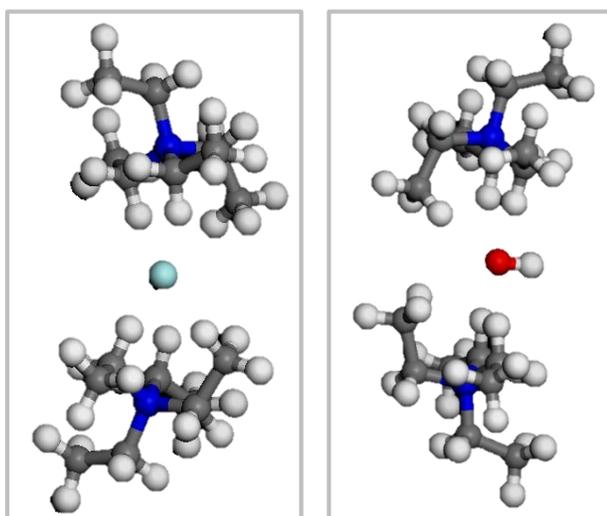
Figure 18. Triple negative structures for tetraethyl phosphonium with fluoride (left) and hydroxide (right)
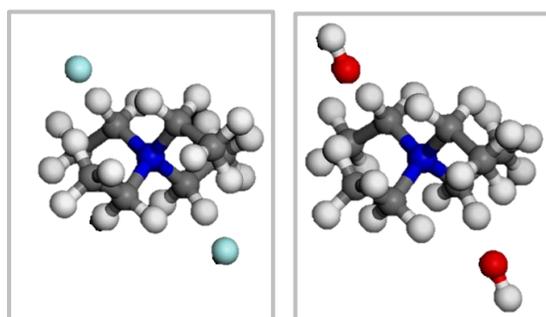
Figure 19. Triple negative structures for tetraethyl ammonium with fluoride (left) and hydroxide (right)

Figure 20. Triple positive structures for tetraethyl phosphonium with fluoride (left) and hydroxide (right)


Figure 21. Triple positive structures for tetraethyl ammonium with fluoride (left) and hydroxide (right)

Triple ion factors exhibit higher preference for the triple ion states for ammonium as compared to phosphonium, likely due to the stronger pairing in phosphoniums over ammoniums. Unlike quadrupole factor comparisons, there are no clear trends in alkyl chain length.
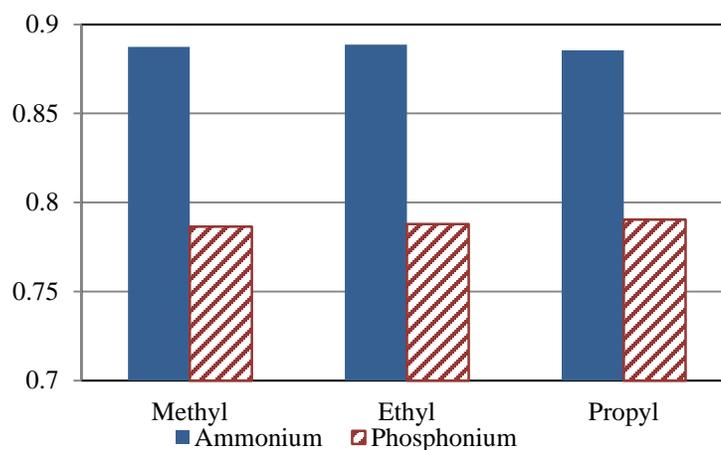
Figure 22. Triple ion factors for fluoride and ammonium or phosphonium with four methyl, ethyl, or propyl substituents.
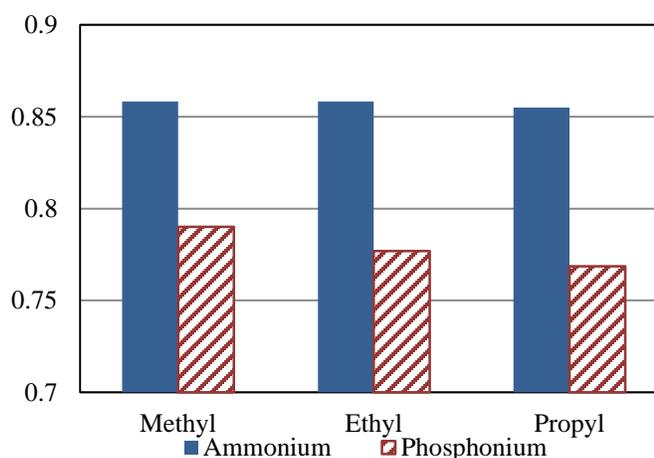

Figure 23. Triple ion factors for hydroxide and ammonium or phosphonium with four methyl, ethyl, or propyl substituents.

Methyl-substituted phosphazenium and phosphazenium with an ethylene glycol chain were also assessed, examining their triple negative (Figure 24) and triple positive (Figure 25) structures. The triple negative structure for phosphazenium with both fluoride and hydroxide adopt the octahedral structure, as compared to phosphonium, which adopts an octahedral structure with hydroxide but not fluoride. This, like the planar paired structure, is a reflection of the electron-withdrawing nature of nitrogen.
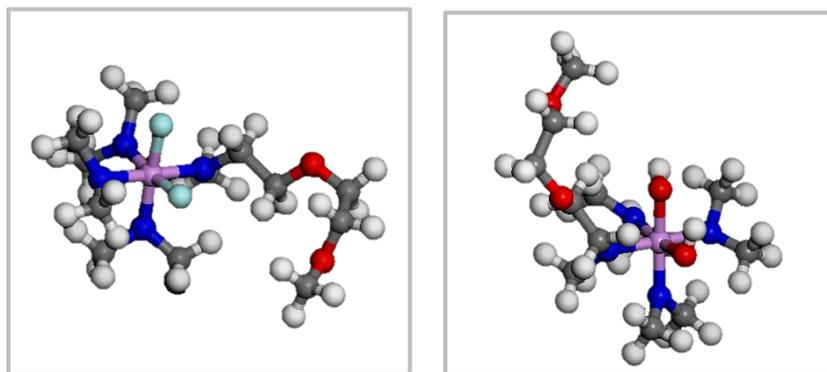
Phosphazenium with an ethylene glycol side chain shows similar structures (Figure 26, Figure 27).
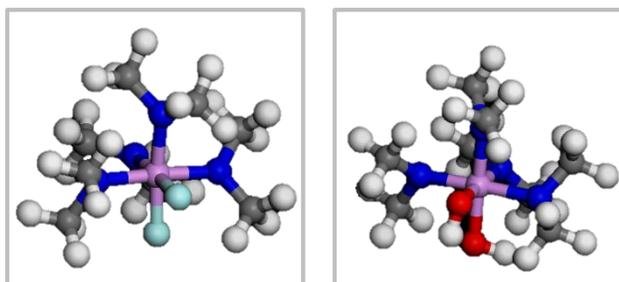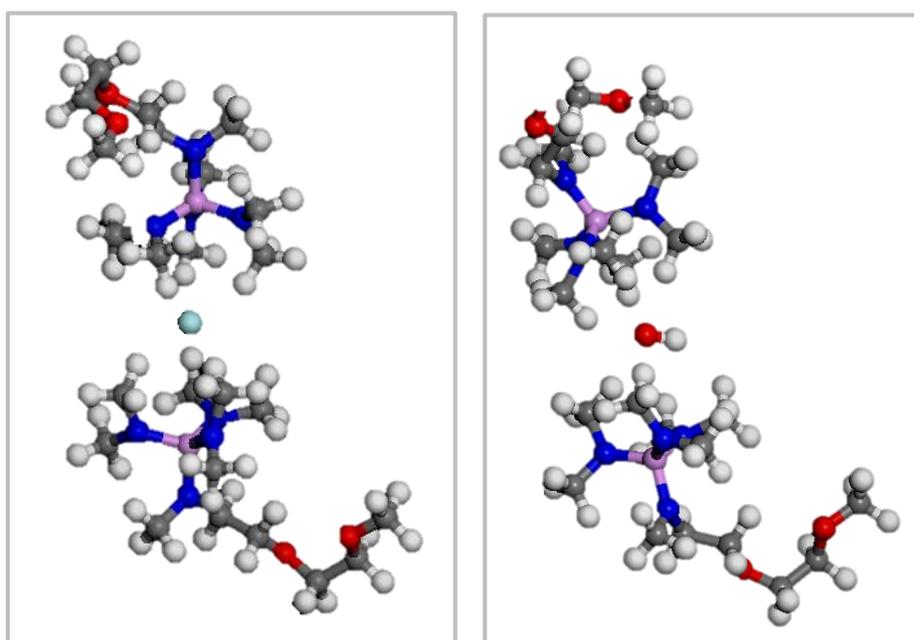

Figure 24. Triple negative structures for phosphazenium with fluoride (left) and hydroxide (right)
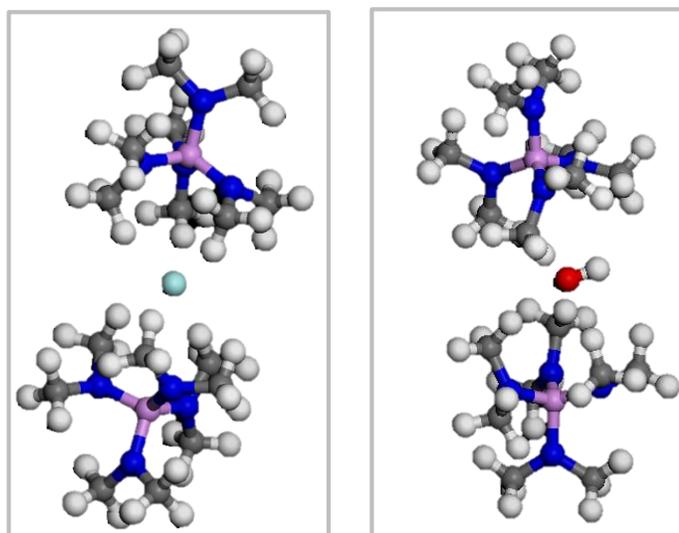
Figure 25. Triple positive structures for phosphazenium with fluoride (left) and hydroxide (right)

Figure 26. Triple negative structures for ethylene glycol-substituted phosphazenium with fluoride (left) and hydroxide (right)


Figure 27. Triple negative structures for ethylene glycol-substituted phosphazenium with fluoride (left) and hydroxide (right)

The triple ion factor for phosphazenium lies between that of phosphonium and ammonium for both fluoride and hydroxide (Figure 28, Figure 29). This holds for each phosphonium or ammonium alkyl chain length tested. The addition of the ethylene glycol chain did not significantly affect the triple ion factor for phosphazenium.
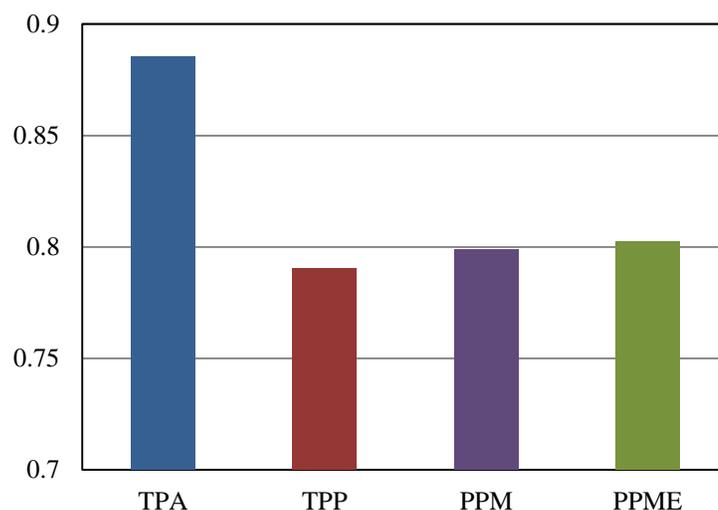
Figure 28. Triple ion factors of fluoride with (left to right) tetrapropyl-ammonium, tetrapropyl-phosphonium, phosphazenium, and phosphazenium with an ethylene glycol side chain.
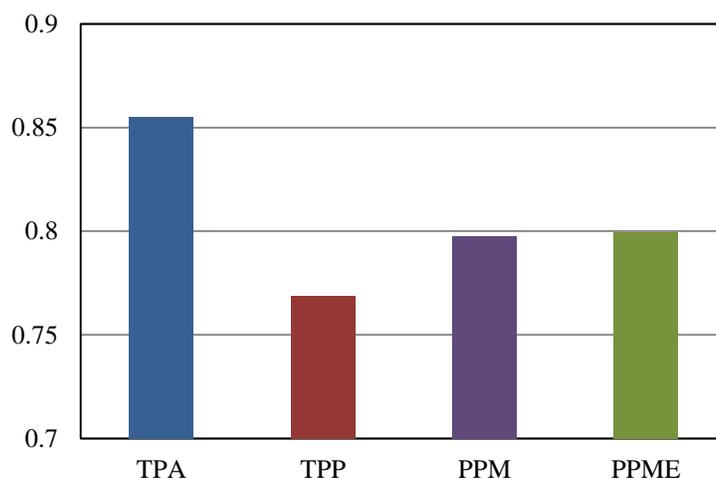

Figure 29. Triple ion factors of hydroxide with (left to right) tetrapropyl-ammonium, tetrapropyl-phosphonium, phosphazenium, and phosphazenium with an ethylene glycol side chain.

A graph of the sum of triple negative and triple positive binding energies versus

three times the pair binding energy graphically displays triple ion factors, shedding light

on previously discussed trends (Figure 30, Figure 31). Triple ion factor decreases

moving farther below the 45 degree line. Triple ion factor for ammonium is highest,

followed by phosphazenium and then phosphonium. The sum of triple ion energies for

phosphazenium is similar to that of tetrapropyl ammonium or phosphonium, while the

pair formation energy for phosphazenium lies between that of phosphonium and

ammonium.   This pair binding energy trend is therefore the main cause for the trend in

decreasing triple ion factor from ammonium to phosphazenium to phosphonium.
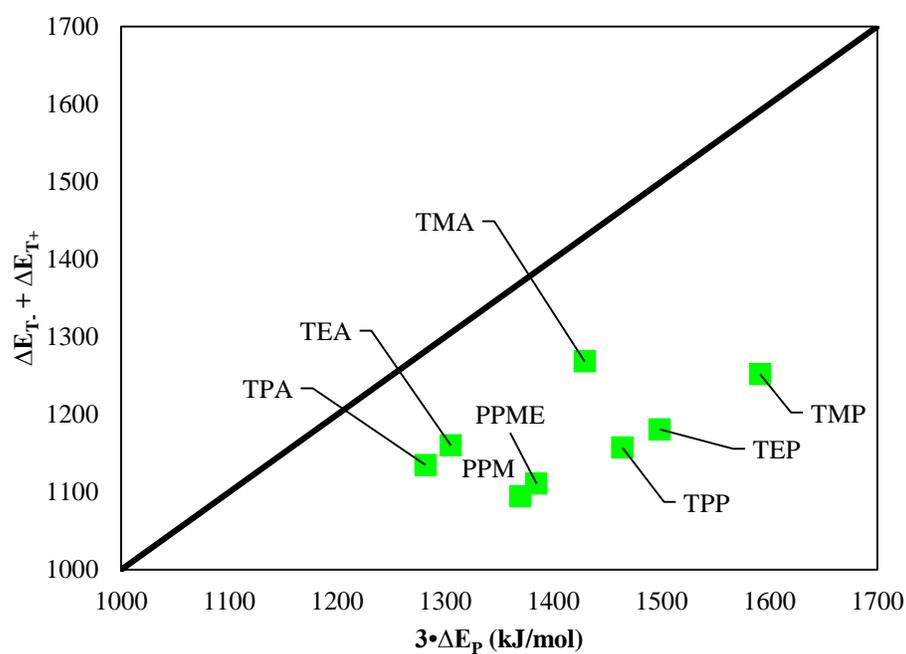
Figure 30. Triple ion factor for cations with F⁻: Formation energy of triple positive and triple negative versus three times the formation energy of the pair
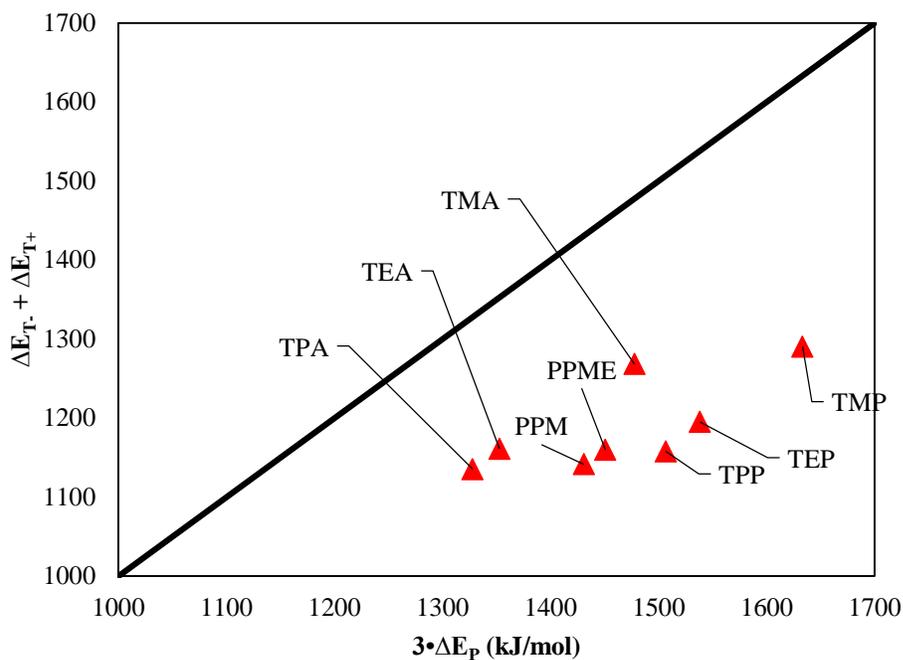
Figure 31. Triple ion factor for cations with OH⁻: Formation energy of triple positive and triple negative versus three times the formation energy of the pair

The triple ion factors indicate that triple ions are more likely to form for the ammonium cations than the phosphonium ions. It is clear that the increased stability of the phosphonium pair due to cationic planarization and closer cation-anion binding is the main contributor. While phosphazenium showed the lowest quadrupole factor, it does not exhibit the lowest triple ion factor; its triple ion factor instead lies between that of phosphonium and ammonium. This suggests that phosphazenium ions may give a better balance of avoiding aggregation (low quadrupole factor) while also allowing for charge species formation (high triple ion factor).
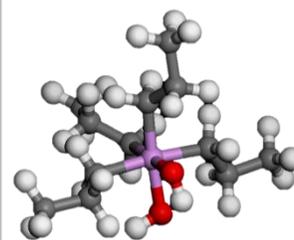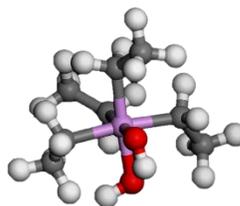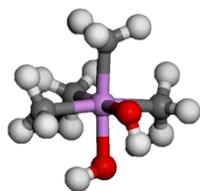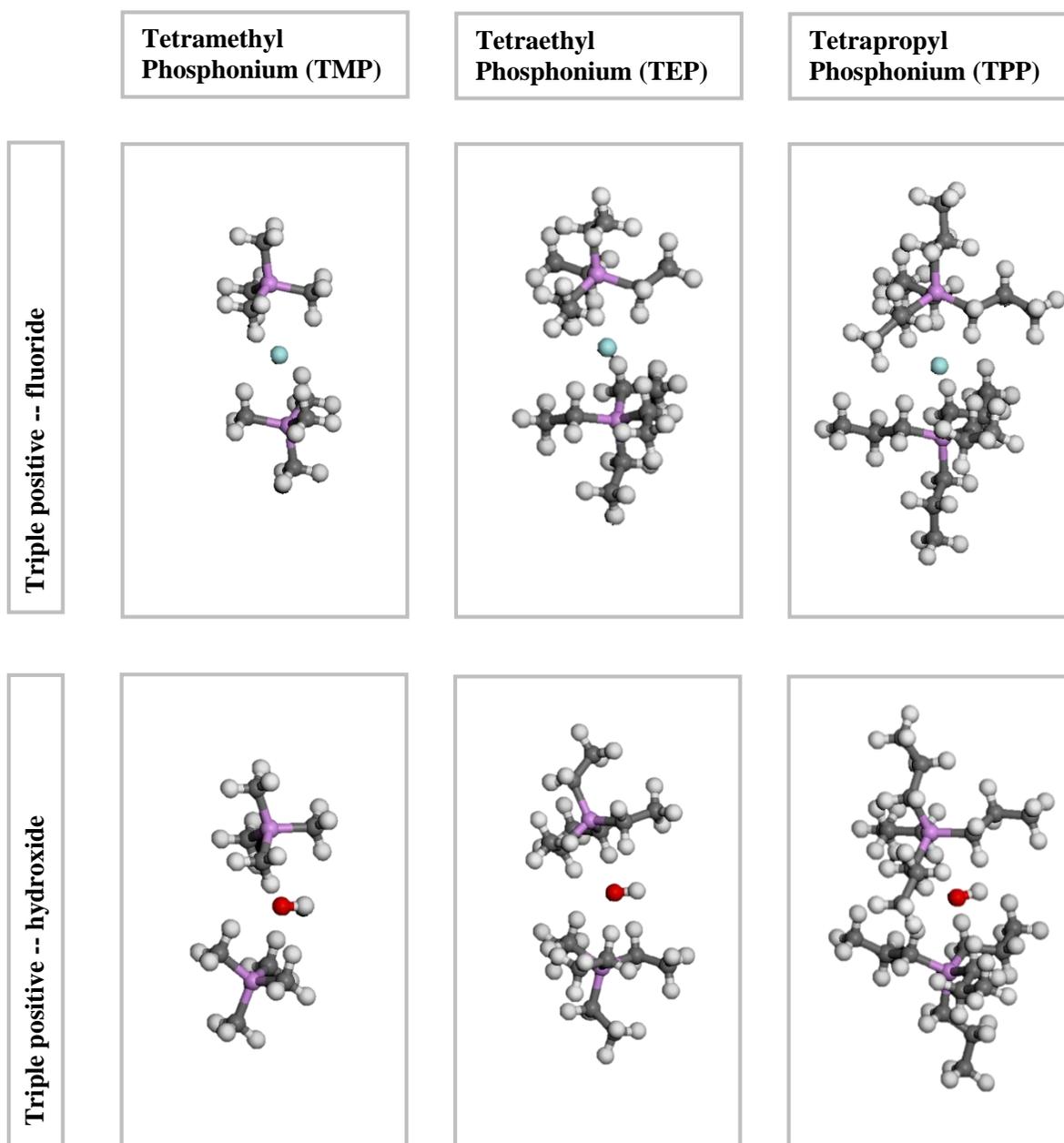
Chapter 4

Conclusions

Calculations of quadrupole factors and triple ion factors shed light into the conductivity of ammonium AEMs versus phosphonium AEMs, and provide support for phosphazenium as an encouraging alternative. Higher triple ion factors of ammonium support the findings of better conductivity as compared with phosphonium, as larger triple ion factors indicate a greater concentration of charged species which promote conduction. The closer bonding between phosphonium and the anion seem to also point to the increased risk for degradation of phosphonium. While phosphonium exhibits quadrupole factors consistently lower than that of ammonium, indicating a smaller tendency to aggregate and form unwanted crosslinks, it also shows smaller triple ion factors, implying that less charge-carrying species are present in ammonium AEMs. Phosphazenium has a quadrupole factor comparable to that of phosphonium while also displaying a larger triple ion factor than phosphonium (though smaller than that of ammonium). Phosphazenium may therefore be a good option for both small crosslink formation risk and existence of charge-carrying species. Cations with similar electron-withdrawing and charge-stabilizing properties, such as tetrabenzyl phosphonium and TPQPOH, may offer similar benefits for AEM conductivity.
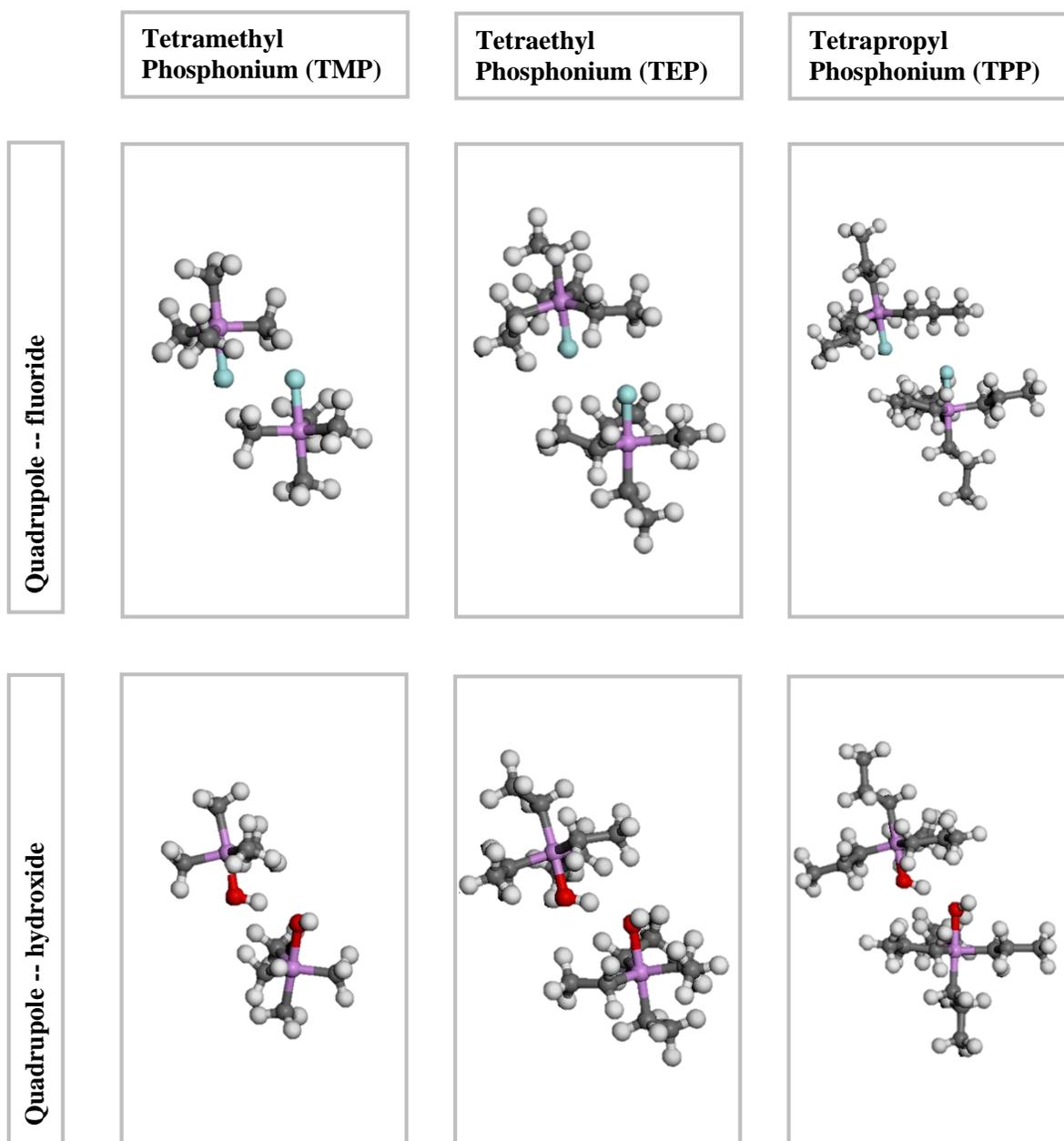
Appendix
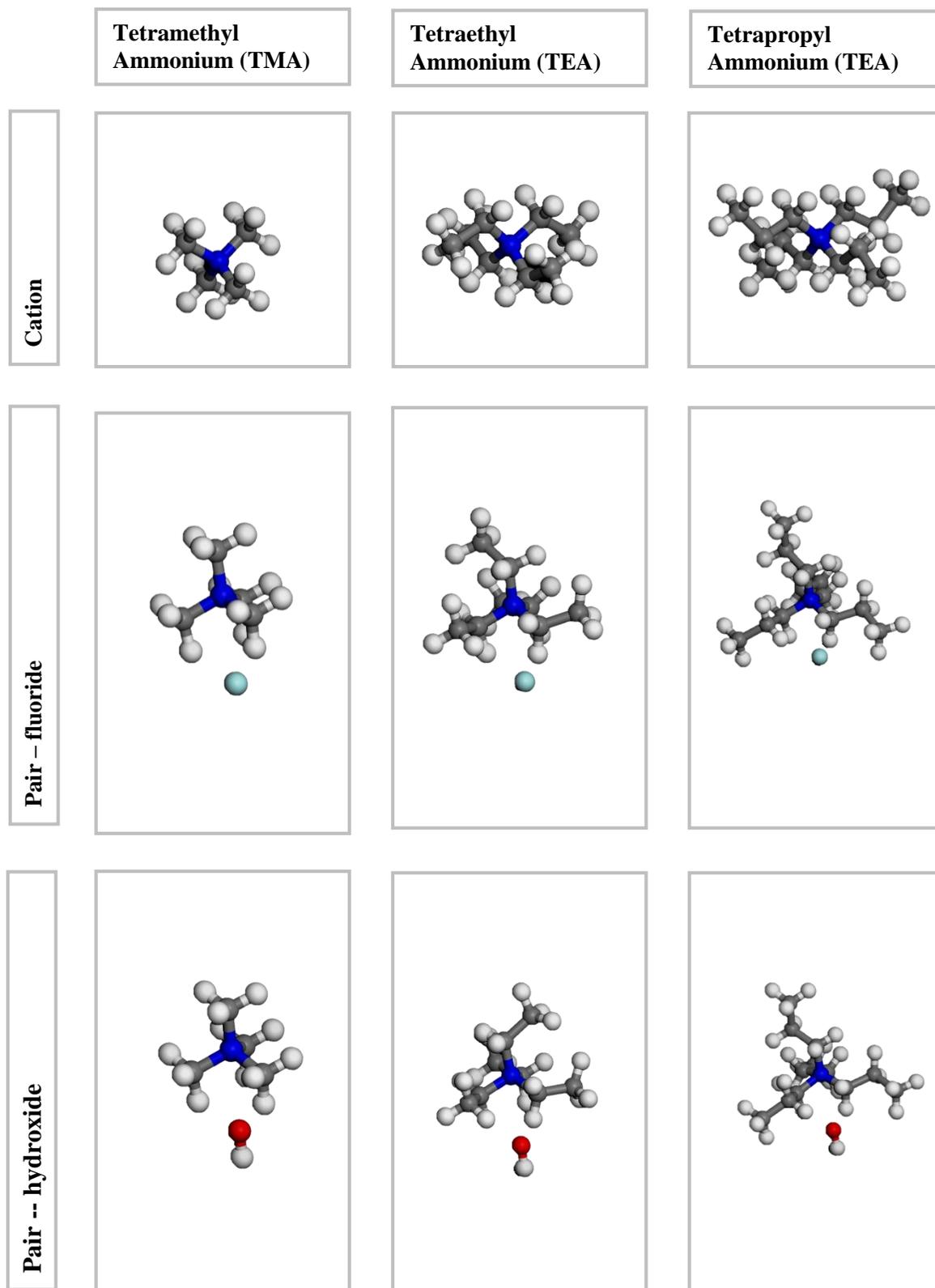
Pictures of lowest-energy structures
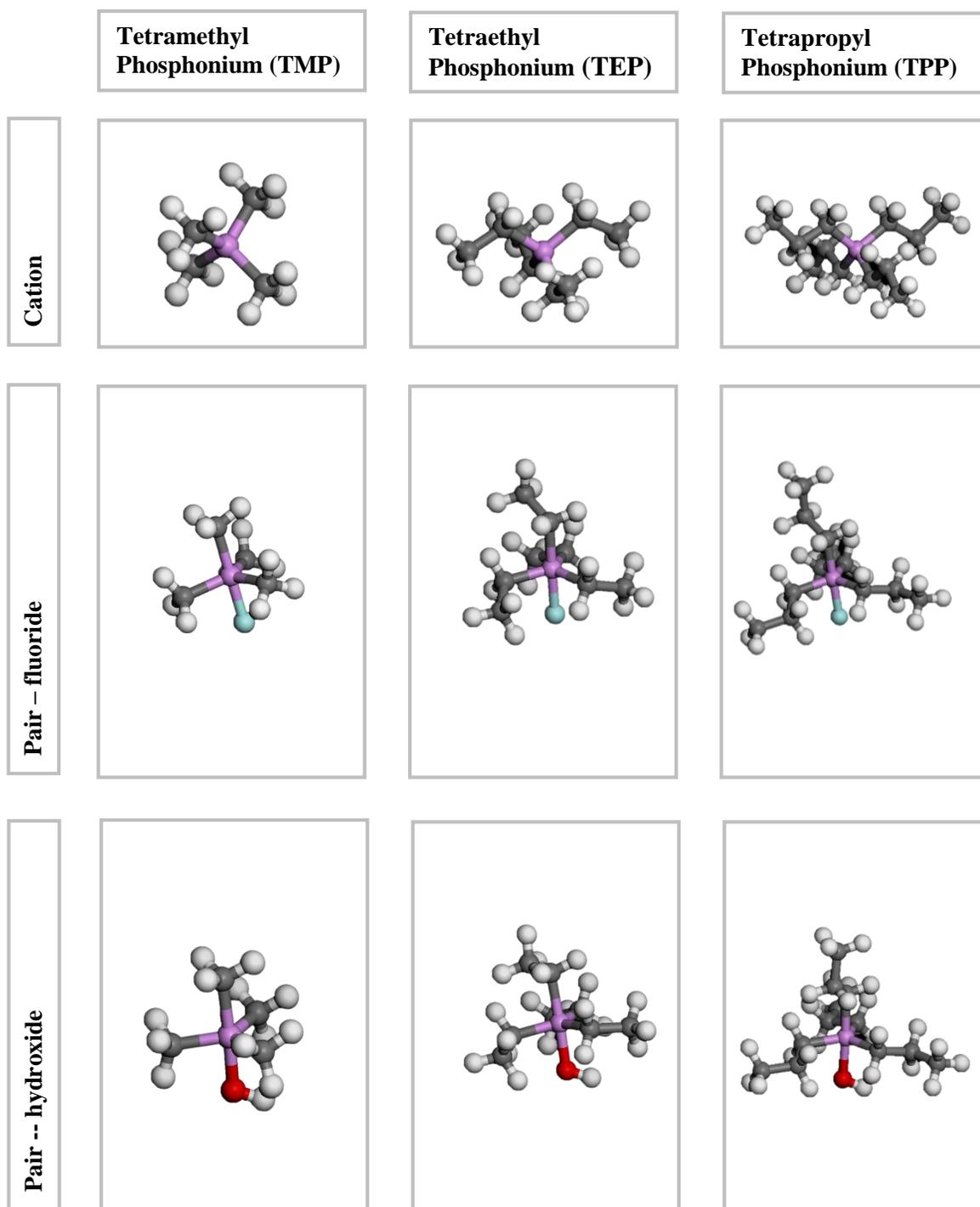
	Tetramethyl Phosphonium (TMP)	Tetraethyl Phosphonium (TEP)	Tetrapropyl Phosphonium (TPP)
Cation			
Pair – fluoride			
Pair -- hydroxide			

Tetramethyl Phosphonium (TMP)	Tetraethyl Phosphonium (TEP)	Tetrapropyl Phosphonium (TPP)

Triple negative -- fluoride
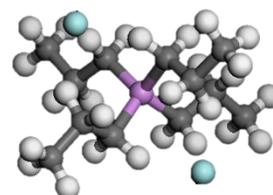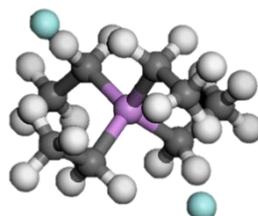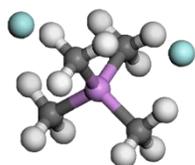
Triple negative -- hydroxide

	Tetramethyl Phosphonium (TMP)	**Tetraethyl Phosphonium (TEP)**	**Tetrapropyl Phosphonium (TPP)**
Triple positive -- fluoride			
Triple positive -- hydroxide			

	Tetramethyl Phosphonium (TMP)	**Tetraethyl Phosphonium (TEP)**	**Tetrapropyl Phosphonium (TPP)**
Quadrupole -- fluoride			
Quadrupole -- hydroxide			

	Tetramethyl Ammonium (TMA)	Tetraethyl Ammonium (TEA)	Tetrapropyl Ammonium (TEA)
Cation			
Pair – fluoride			
Pair -- hydroxide			

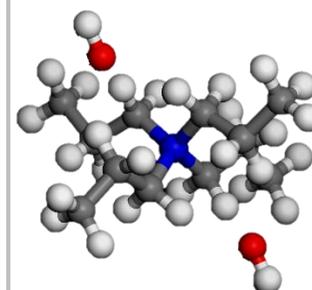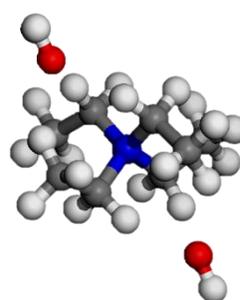|	Tetramethyl Ammonium (TMA)	Tetraethyl Ammonium (TEA)	Tetrapropyl Ammonium (TPA)
Triple negative -- fluoride			
Triple negative -- hydroxide			
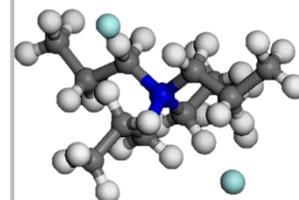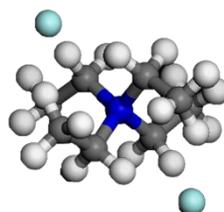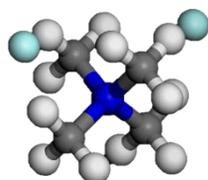
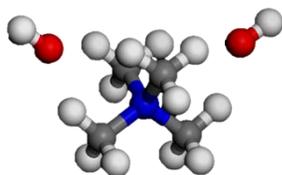|	**Tetramethyl Ammonium (TMA)**	**Tetraethyl Ammonium (TEA)**	**Tetrapropyl Ammonium (TPA)**
Triple positive -- fluoride			
Triple positive -- hydroxide			

	Tetramethyl Ammonium (TMA)	Tetraethyl Ammonium (TEA)	Tetrapropyl Ammonium (TPA)
Quadrupole -- fluoride			
Quadrupole -- hydroxide			

	Phosphazenium (PPM)	**Phosphazenium, ethylene glycol (PPME)**
Cation		
Pair – fluoride		
Pair -- hydroxide		

43
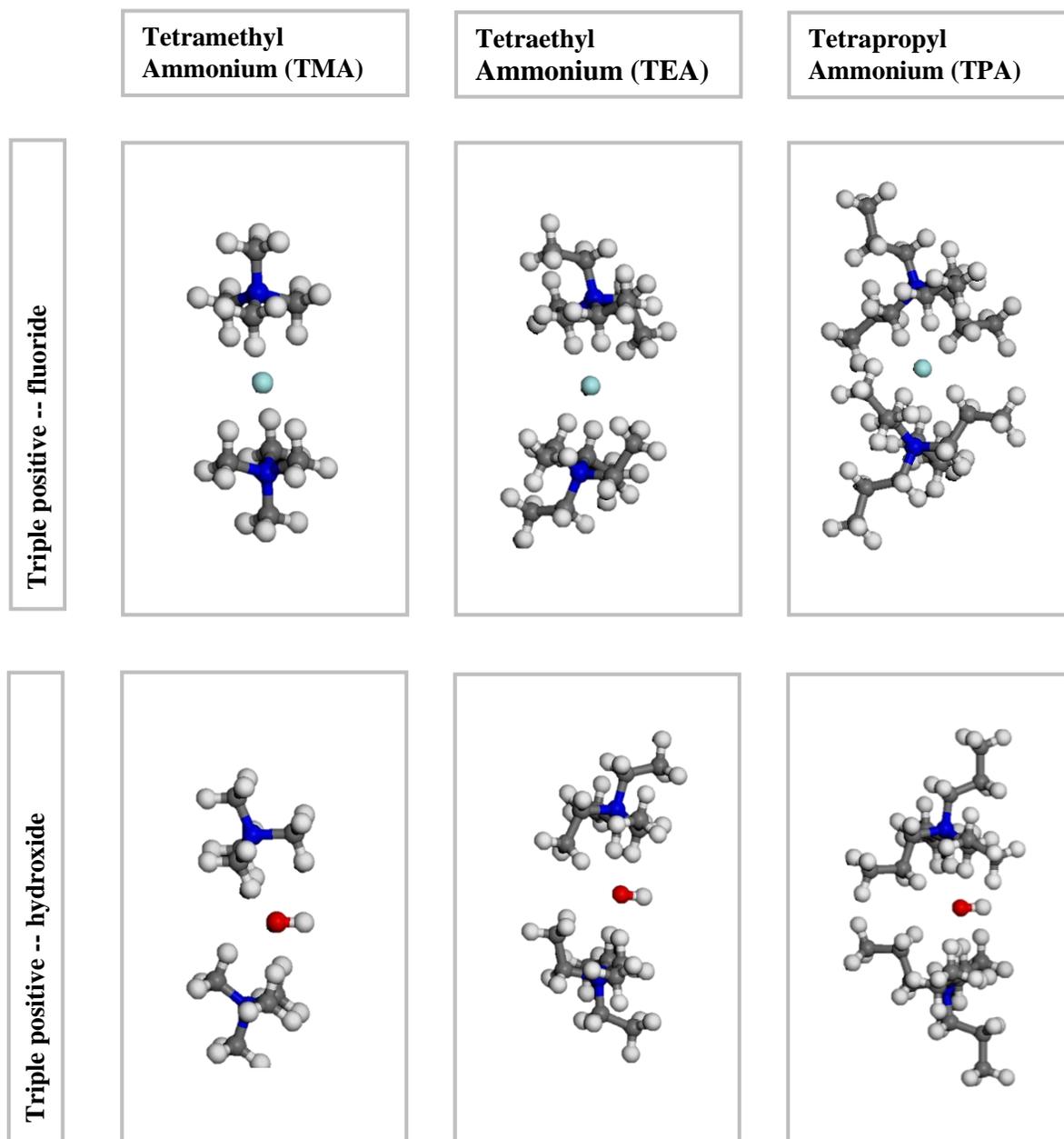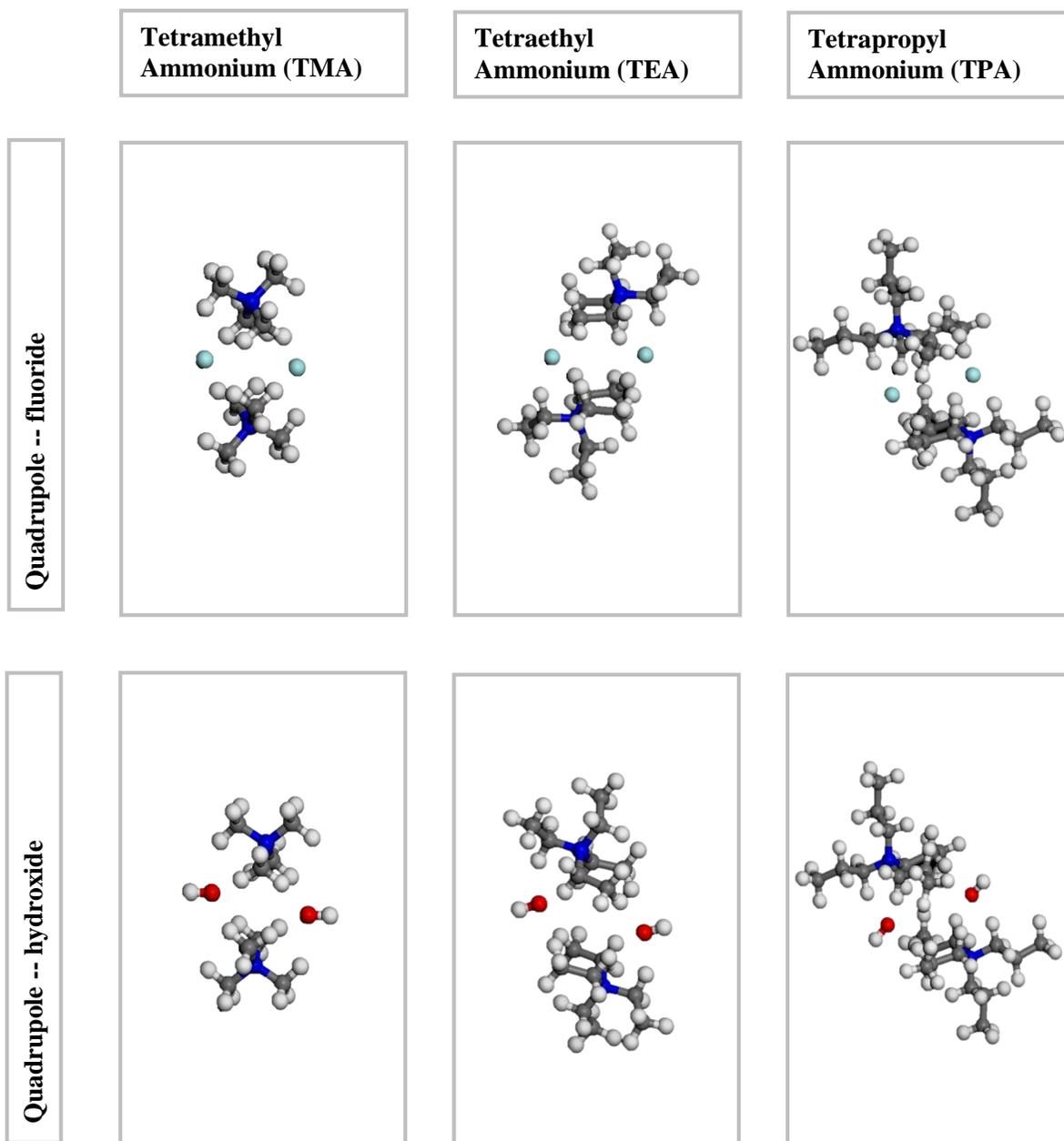
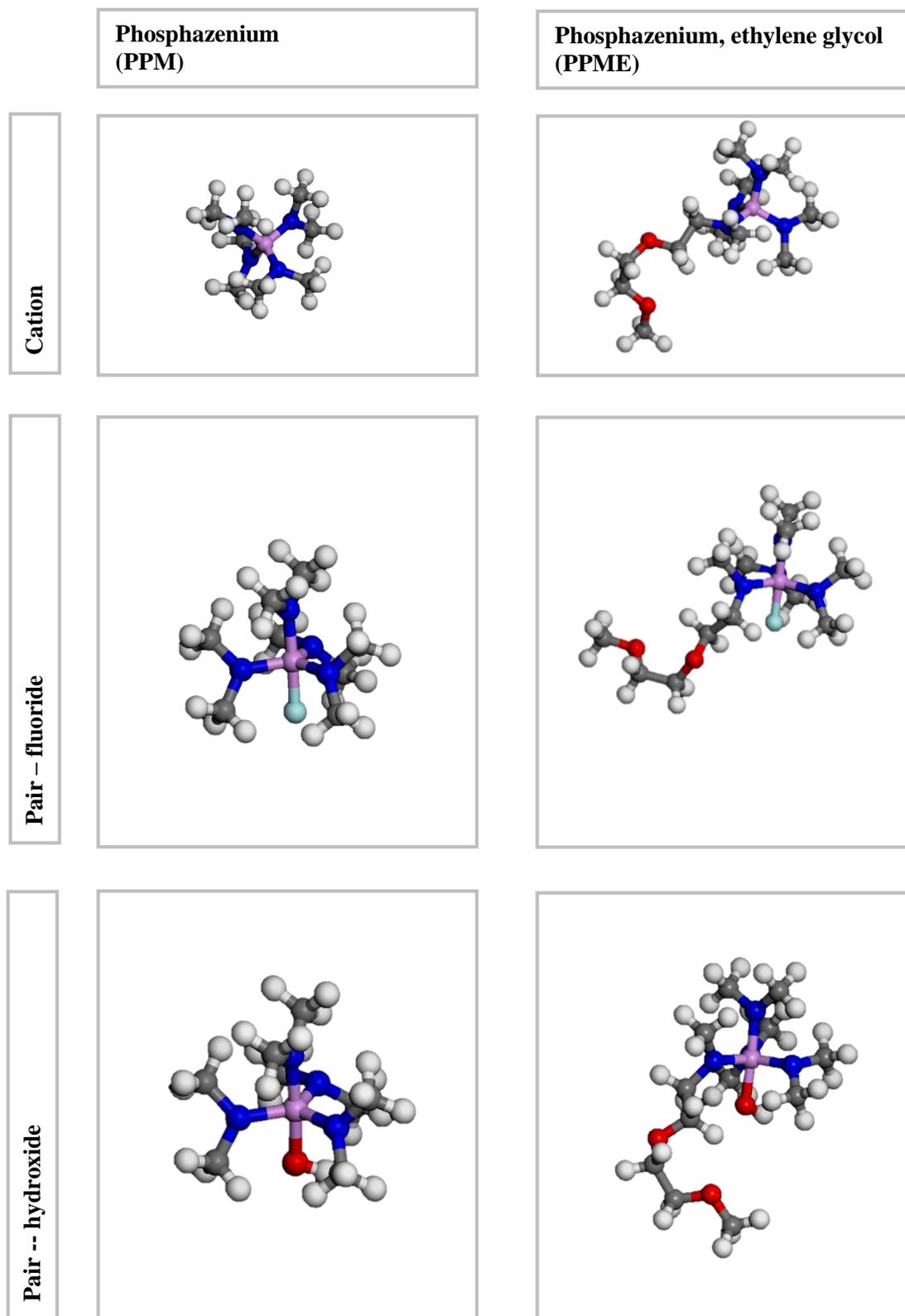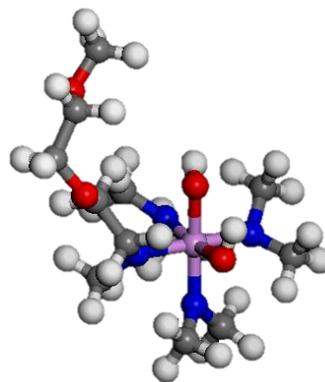| Phosphazenium (PPM)	Phosphazenium, ethylene glycol (PPME)
Triple negative – fluoride		
Triple negative -- hydroxide		
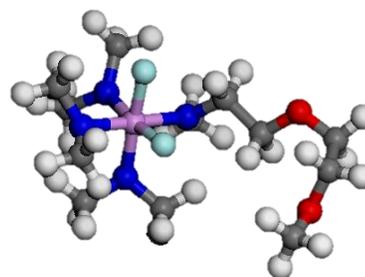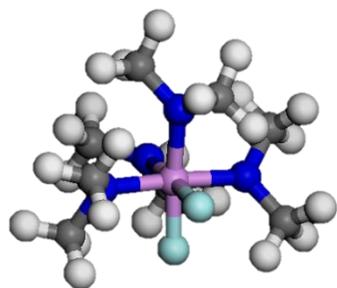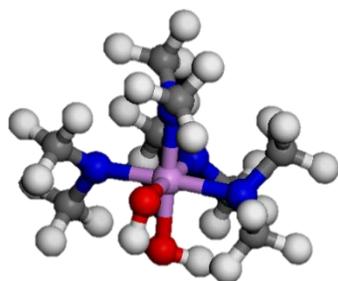
Phosphazenium (PPM)	Phosphazenium, ethylene glycol (PPME)

Triple positive – fluoride		
Triple positive -- hydroxide		
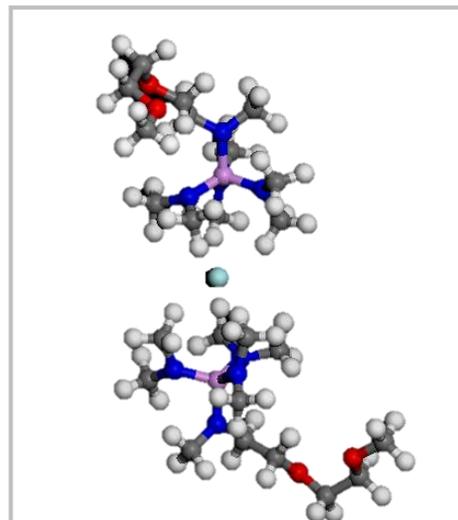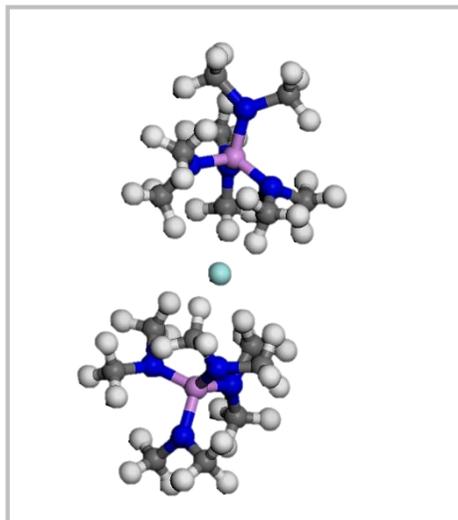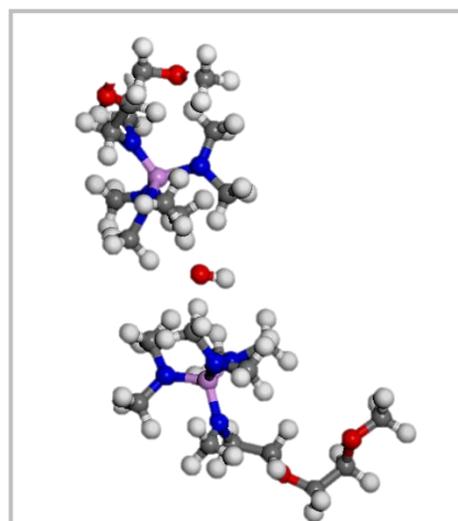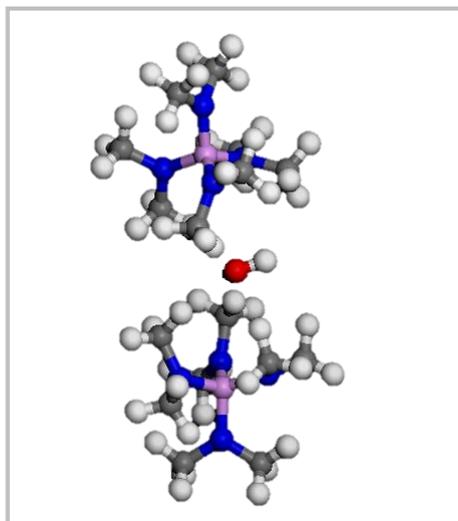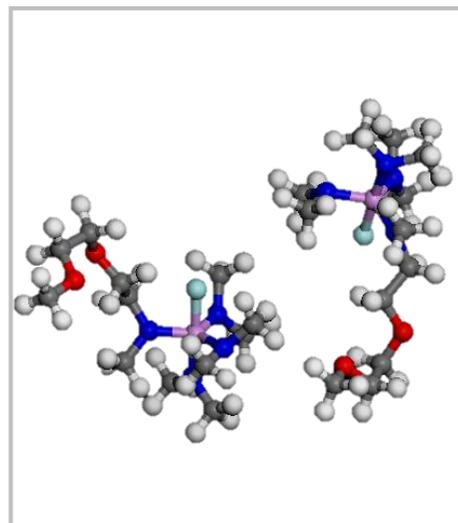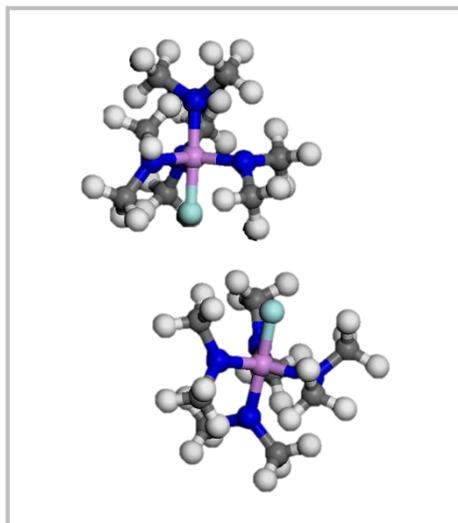
Phosphazenium (PPM)	Phosphazenium, ethylene glycol (PPME)
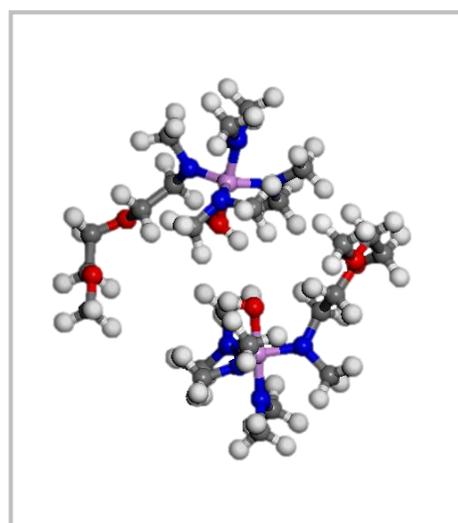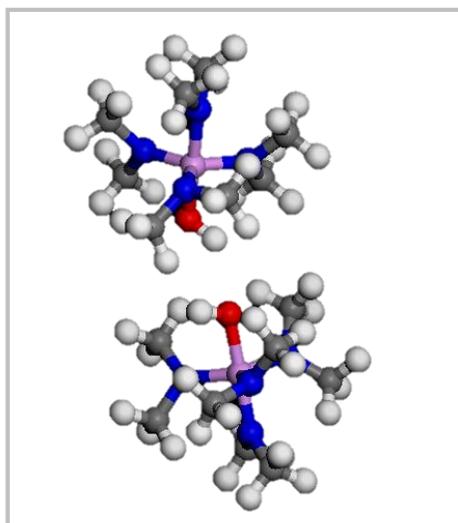
Bibliography

[1] Arges, C. G., Ramani, V., & Pintauro, P. N. (2010). Anion Exchange Membrane Fuel Cells. *The Electrochemical Society Interface*, 31-35.

[2] Chempath, S., Einsla, B. R., Pratt, L. R., Macomber, C. S., Boncella, J. M., Rau, J. A., & Pivovar, B. (2008). Mechanism of tetraalkyl headgroup degradation in alkaline fuel cell membranes. *The Journal of Physical Chemistry*, 3179-382.

[3] Couture, G., Alaaeddine, A., Boschet, F., & Ameduri, B. (2011). Polymetric materials as anion-exchange membranes for alkaline fuel cells. *Polymer Science*, 1521-1557.

[4] Deavin, O., Murphy, S., Ong, A. L., Poynton, S. D., Zeng, R., Henryk, H., & Varcoe, J. R. (2012). Anion exahcne membranes for alkaline polymer electrolyte fuel cells: comparison of pendent benzyltrimethylammonium- and benzyltrimethylimidazoleym-head-groups. *Energy and Environmental Science*, 8584-8597.

[5] Gu, S., Cai, R., Luo, T., Jensen, K., Contreras, C., & Yan, Y. (2010). Quaternary phosphonium-based polymers as hydroxide exchange membranes. . *ChemSusChem*, 555-558.

[6] Liu, W., Janik, M. J., & Colby, R. H. (2012). Polyelectrolytes for Batteries and Fuel Cells. *Polymers for Energy Storage and Delivery*, 19-44.

[7] Reddy, M. A., & Fichtner, M. (2011). Batteries based on fluoride shuttle. *Journal of Materials Chemistry*, 17059-17062.

[8] Salerno, H., Beyer, F., & Elabd, Y. (2012). Alkaline exchange membranes derived from Nafion precursor for the alkaline fuel cell. *Journal of Polymer Science*, 552-562.

[9] Shiau, Huai-Suen; Liu, Wenjuan; Colby, Ralph; Janik, Michael J. (2013). Cluster-continuum quantum mechanical models to guide the choice of anions for Li+-conducting ionomors. *Journal of Chemical Physics*

[10]   Unlu, M., Zhou, J., & Kohl, P. A. (2009). Anion Exchange Membrane Fuel Cells: Experimental Comparison of Hydroxide and Carbonate Conductive Ions. *Electrochemical and Solid-State Letters*, B27.

[11]   Zarrin, H., Wu, J., Fowler, M., & Chen, Z. (2012). Highly durable PEK-based anion exchange membrane for elevated temperature alkaline fuel cells. *Journal of Membrane Science*, 193-201.

[12]   Zha, Y., Disabb-Miller, M. L., Johnson, Z. D., Hickner, M. A., & Tew, G. N. (2012). Metal-cation-based anion exchange membranes. *JACS*, 4493-4496.

ACADEMIC VITA

Nicole LaBarge
106 Windy Hollow Dr., Phoenixville, PA 19460
_____

Education

B.S., Chemical Engineering, 2014; Minors in Chemistry and Environmental Engineering
The Pennsylvania State University, Schreyer Honors College

Honors and Awards

Penn State REU in Chemical Engineering   Summer 2012
Best Design Communication, Engineering Design Showcase   Fall 2011
Schreyer Honors College Academic Excellence Scholarship   Fall 2010 – Spring 2014

Association Memberships/Activities

Science Lions; President
- Organize demonstrations to foster K-12 interest in science and engineering
- Developed new Gas Laws and Oil Spill shows
- Served as Vice President (2011 – 2012) and Secretary (2010 – 2011)

Ballroom Dance Club; Salsa teacher and coordinator
- Coordinate and teach lessons for 100 students and faculty members
- Develop guidelines for teaching lessons and training new teachers
- Served as Public Relations Chair (*2011 – 2012*) and Salsa Coordinator (*2010 – 2011*)

Professional Experience

Undergraduate Research Assistant; Spring 2012 – Spring 2014
- Analyze cations to improve conduction within anion exchange membranes under the direction of Dr. Janik and Dr. Colby
- Perform quantum mechanical testing to assess cation affinity for pairing and aggregate formation

Applications Engineering Intern, Brentwood Industries; Summer 2013
- Designed trickling filter systems for wastewater treatment upgrades, including a 42 MGD facility
- Developed charts and presentation material emphasizing product capabilities for innovative biological treatment system
- Created a presentation addressing concerns of media plugging